Journal of Hazardous Materials 211–212 (2012) 55–61

Contents lists available at SciVerse ScienceDirect

Journal of Hazardous Materials

journal homepage: www.elsevier.com/locate/jhazmat

Bioinspired synthesis of hierarchically micro/nano-structured CuI tetrahedron and its potential application as adsorbent for Cd(II) with high removal capacity

Shuyan Gao [a,*], Jianmao Yang [b], Zhengdao Li [a], Xiaoxia Jia [a], Yanli Chen [a]

[a] College of Chemistry and Environmental Science, Henan Normal University, 46 Jianshe Street, Xinxiang, 453007, Henan, PR China
[b] Research Center for Analysis and Measurement, Donghua University, Shanghai, 201620, PR China

ARTICLE INFO

Article history:
Received 1 June 2011
Received in revised form
10 December 2011
Accepted 3 January 2012
Available online 11 January 2012

Keywords:
Adsorbent
Cd(II) ions
CuI
Green chemistry
Hierarchical micro/nano-structure

ABSTRACT

An environment friendly bioinspired strategy for synthesizing hierarchically micro/nano-structured CuI tetrahedron has been developed by combining the stabilization and the reduction performances of L-tryptophan together. A possible growth mechanism of such hierarchical tetrahedron is tentatively proposed. Remarkably, such CuI tetrahedron is found to possess high removal capacity for poisonous Cd(II) ions, 136.3 mg/g, and ideal reusability. This is ascribed to the hierarchical micro/nano-structure and chemical adsorption mechanism, which shows great advantages over the traditional nano-scaled adsorbents. These interesting results stand out the promising applications of such hierarchically micro/nano-structured materials in environment. It is also a good example for the organic combination of green chemistry and nanotechnologies for the treatment of contaminated water.

1. Introduction

Rapid industrialization comes as a negative consequence of environmental pollution which in turn affects human health [1–3]. Heavy metals discharged from industrial processes (such as metal plating, electroplating, metal finishing, mining, battery, pigment, dyestuff, paint, etc.) and into natural water can differently affect the biological behavior of aquatic organisms and physiological phenomena of human beings according to the type of the element and the chemical form of dissolved species [4,5]. As it is widely known, Cd(II) is very toxic [6], prolonged exposure to which causes kidney failure, anemia, cardiovascular diseases, growth impairment, and loss of taste and smell [7]. For these reasons, environmental regulations define severe limitations on the maximum Cd concentration in natural water bodies as well as on the maximum allowed concentration for wastewater discharge [8]. To assure the compliance with these limits, appropriate depuration technologies are consistently required so that various techniques have been employed such as membrane filtration, ion-exchange, solvent extraction, chemical precipitation, reverse osmosis, cementation, electrodialysis, electrocoagulation, adsorption, etc. [8–20] to alleviate the problem of water pollution by Cd(II) in the environment. Among the available remedial technologies, adsorption is popular because of its low cost and simplicity [21–27]. Recently, nanomaterials are receiving more and more attention as adsorbents for the removal of heavy metals from water [8], and therefore, it seems reasonable to search for nanomaterials as adsorbents. However, in general, nanomaterials tend to be less stable and prone to aggregation to minimize their surface area due to their higher surface energy, resulting in a remarkable reduction in their adsorption activities. An available way to prevent the nanoparticles from aggregation and maintain the high efficiency is to organize these nanometer-scaled materials into a hierarchical structure [28]. So it is interesting and significant to develop adsorbents with hierarchical structures for improved removal capacity for poisonous Cd(II) ions.

It is widely realized in all of biology, chemistry, and materials science that biomolecules' special structures and strong assembling functions can be utilized to fabricate complicated functional nanocrystals with desired shape from a single functional structure [29–31]. Tryptophan is one of the 20 standard amino acids, as well as an essential amino acid in the human diet. Inspired by the biomolecules-directed inorganic material synthesis [32–35], we hypothesize that tryptophan can provide the scaffolds necessary to interact with and sequester the inorganic ions. Herein, we take CuI as an example to demonstrate biomolecule-assisted green method for synthesizing hierarchically micro/nano-structured CuI tetrahedron assembling from nanosheets simply by using L-tryptophan as mild reductant and excellent morphology-directing agent. In comparison with the reported protocols, our method is a green,

* Corresponding author. Tel.: +86 373 3326335; fax: +86 373 3326544.
E-mail address: shuyangao@htu.cn (S. Gao).

0304-3894/$ – see front matter © 2012 Elsevier B.V. All rights reserved.
doi:10.1016/j.jhazmat.2012.01.016

environment-friendly, time-saving, and direct one-step process. Compared to nano-sized materials, the hierarchical micro/nano-structure can effectively maintain the structure and mechanical stability, thus avoiding the aggregation and deconstruction, and, moreover, guaranteeing the recycle performance. As a demonstration, the synthesized hierarchically micro/nano-structured CuI is tested for removing Cd(II) from water and shows high and recyclable removal capacity. This preliminary investigation emphasizes the advantage of hierarchically micro/nano-structure over the bulk and nano-sized counterparts, which places solid foundation for the feasible and promising application of such materials in adsorption. What is worth mentioning is that the chemical adsorption mechanism as well as hierarchical micro/nano-structure plays a vital role in the excellent Cd(II) removal performance.

2. Experimental

2.1. Synthesis of tetrahedral CuI

All chemical reagents were of analytical grade and used without further purification. The water used in this investigation was deionized by a nanopure filtration system to a resistivity of 18 MΩ cm. The preparation of L-tryptophan-assisted hierarchically tetrahedral CuI micro/nano-structures is quite straightforward. Twenty-one milliliter of 0.15 M $CuSO_4$ aqueous solution, 35 mL of 0.005 M L-tryptophan aqueous solution, and 21 mL of 0.15 M KI aqueous solution were added under constant stirring, respectively, to 133 mL of ultrapure water. The mixture was stirred for 10 min at room temperature to prepare the CuI sample. When the reaction was completed, gray precipitate and colorless supernatant were obtained. The resulting precipitate was filtered and washed with distilled water and finally dried in air naturally. The yield is ~72%.

2.2. Sample characterizations

X-ray diffraction (XRD) measurement was recorded in the 2θ range of 20–80° on a Rigaku-D/Max 2500V/PC X-ray diffractometer using Cu Kα1 radiation (λ = 1.54056 Å) at 40 kV and 200 mA. Field emission scanning electron microscopy (FESEM) images were obtained on an XL30 ESEM FEG scanning electron microscopy operating at 20 kV. Transmission electron microscopy (TEM) and high-resolution transmission electron microscopy (HRTEM) images were taken on a JEOL 2010 transmission electron microscope. Elemental composition was analyzed by an ESCALab MKII X-ray photoelectron spectrometer, equipped with a monochromatized Mg Kα X-ray as excitation source. Cd(II) concentration in metal ion adsorption test was detected using atomic absorption spectrophotometer.

2.3. Metal ion adsorption test

The as-obtained CuI sample was tested for Cd(II) removal using batch technique. Solutions of various Cd(II) concentrations were obtained by diluting a Cd(II) standard solution of 1000 mg/L. All adsorption experiments were carried out using Erlenmeyer flasks (50 mL). Control experiments showed that no sorption occurred on the container wall. In the adsorption experiment, 0.015 g of CuI was thoroughly mixed with 10 mL of each of Cd(II) solutions. After the mixture was agitated for 3 h and then placed for 1 h to establish equilibrium at room temperature, the CuI powder was then separated from the mixture by centrifugation. The supernatant was analyzed for Cd(II) concentration using atomic absorption spectroscopy (AAS). The isotherm studies were carried out at different initial Cd(II) concentrations between 100 and 900 mg/L. The

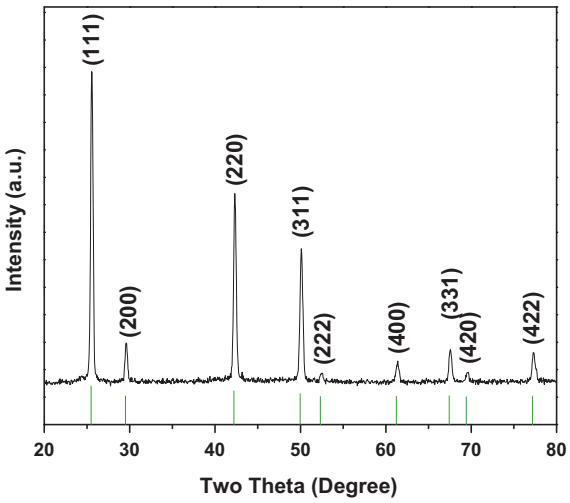

Fig. 1. Typical XRD pattern of the sample. The vertical lines represent the data of JCPDS card no. 06-0246.

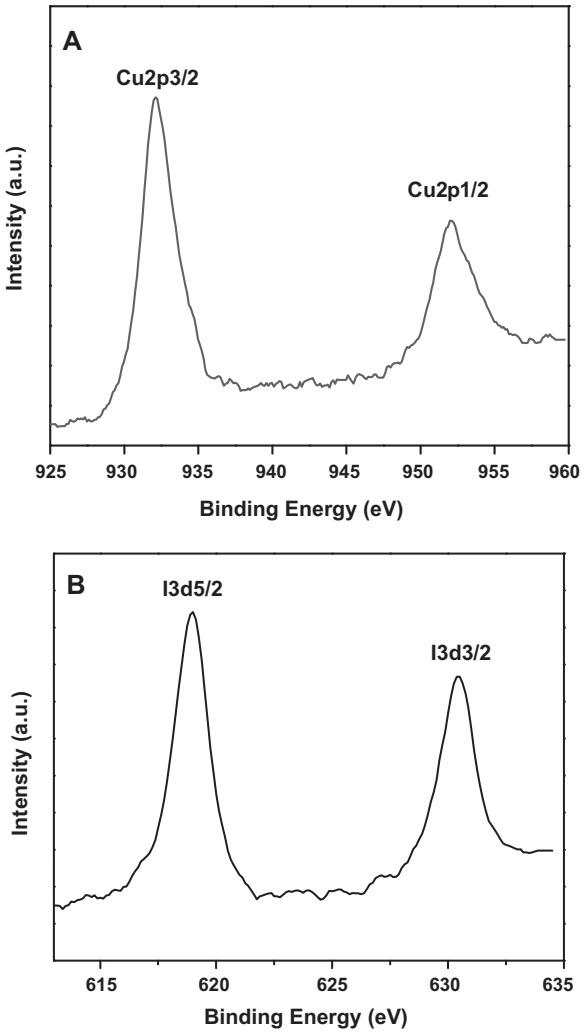

Fig. 2. High-resolution XPS spectra taken for the Cu and I region of the CuI sample: (A) Cu 2p, (B) I 3d5.

amount of Cd(II) adsorbed per unit mass of CuI (Q_e) was calculated by the difference between the initial and the final readings using the following Eq. (1):

$$Q_e = \frac{(C_i - C_e)V}{M} \quad (1)$$

Here, C_i is initial concentration of metal ion in solution (mg/L), C_e is equilibrium concentration of cadmium ion (mmol/L or mg/L), V is volume, M is mass of the adsorbent (g), and Q_e is amount adsorbed per unit mass of adsorbent (mmol/g or mg/g), respectively [36]. Adsorption/desorption cycles were performed to examine the reusability and metal recovery efficiency of the adsorbent CuI. Each cycle consisted of loading with an aqueous Cd(II) solution (C_0 = 100 mg/L) and elution of the bound Cd(II) with 10 mL of 0.001 M EDTA (abbr. Y) solution for 3 h. The desorbed Cd(II) was collected and estimated using AAS. The desorption ratio (Dr) was calculated using the following Eq. (2):

$$\mathrm{Dr} = \frac{\text{amount of metal desorbed to the elution medium}}{\text{amount of metal absorbed on the adsorbent}} \times 100\% \quad (2)$$

The regenerated adsorbent CuI was again tested for further adsorption of Cd(II). Adsorption and desorption experiments were repeated for 3 cycles.

3. Results and discussion

3.1. Structural analysis of CuI sample

The XRD pattern of the as-prepared sample (Fig. 1) is in good agreement with the standard data of single cubic phase CuI with

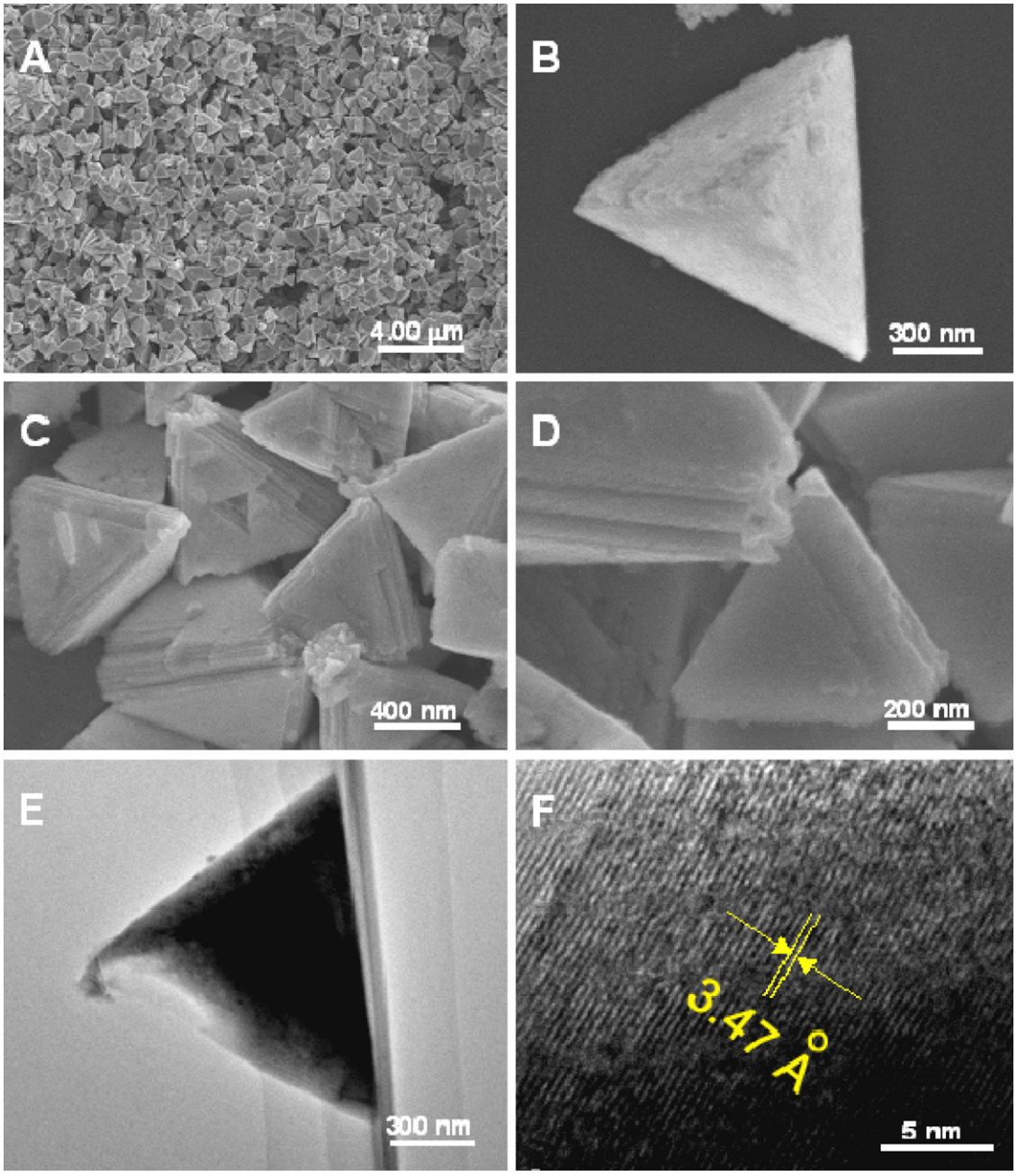

Fig. 3. FESEM images of the sample: (A) low-magnification image, (B) a single tetrahedron, (C) and (D) crashed CuI nanostructure, (E) TEM image, and (F) HRTEM image.

a Marshite, syn structure (JCPDS 06-0246). The fact that no other characteristic diffraction peaks arising from metallic Cu or Cu oxides appear in the XRD pattern indicates a well-crystallized high-purity product was prepared via the bioinspired synthesis process. The extremely strong reflection peaks of (2 2 0), (1 1 1) planes and the seriously suppressed reflection peaks of (2 0 0) and (4 0 0) planes can be easily observed. To obtain chemical states of the elements within the sample, we performed detailed analysis of X-ray photoelectron spectroscopy (XPS) spectra. The binding energies were corrected for specimen charging by calibrating the C 1s peak to 284.6 eV. Fig. 2A shows that the positions of the peaks of Cu $2p_{1/2}$ and $2p_{3/2}$ of the sample CuI are 952.1 and 932.1 eV with no shakeup, which would imply a feature of Cu^{+} [37]. As shown in Fig. 2B, the binding energies of I $3d_{5/2}$ is 619.0 eV, which indicates that I is present in the form of I^{-} assigned to CuI [17]. And there is no the existence of I_2, because the binding energies of I $3d_{5/2}$ in the form of I_2 is above 620 eV [38,39]. In addition, corresponding to XPS analysis, the atomic ratio of copper and iodine was 1:1 approximately. Therefore, the XPS results further prove that the sample is composed of CuI.

In order to obtain detailed information about the microstructure and morphology of the as-synthesized sample, FESEM observations are carried out and shown in Fig. 3A–D. The low-magnification image (Fig. 3A) indicates that the panoramic morphology of the as-prepared sample is mainly composed of uniform tetrahedra ranging from 0.8 to 1.2 μm in edge. The clear view of Fig. 3B displays that the surface of the tetrahedral architectures is not smooth. The examination of a crashed tetrahedron (Fig. 3C and D) vividly reveals that the structure of these tetrahedral architectures is assembled from nanosheets with average thickness of ca. 15 nm. The microstructure of the as-grown sample is further analyzed using TEM and HRTEM. TEM image of a single crystal (Fig. 3E) reveals clearly the tetrahedral morphology. The length of the side is around 0.9 μm. The HRTEM image in Fig. 3F can give further insight into the details of the structure. The lattice fringes can be clearly distinguished, which indicates its single-crystalline nature and the *d* spacing of 3.47 Å correspond to the {1 1 1} plane. This result is consistent with the XRD pattern.

3.2. Growth mechanism

What is the underlying growth mechanism for such hierarchically micro/nano-structured tetrahedron? Generally, the selective adsorption of surfactants, ions, ligands, or polymers on a given crystal plane can inhibit the crystalline growth along one specific direction, leading to a preferential growth along another direction [40–42]. Therefore, the introduction of an additive with a selective adsorption function is widely used for the synthesis of anisotropic nanocrystals in a solution phase. In our system, how does L-tryptophan help the formation of such hierarchically micro/nano-structured tetrahedron? What is the driving force? Let us tentatively explain it (Scheme 1). The formation mechanism should be considered from three aspects. First, it is believed that the growth of tetrahedron should be completed by two steps, i.e. the formation of nanosheets and their subsequent self-assembly process, respectively. In our biomolecule-assisted route, the L-tryptophan plays a crucial role in the shape control of nanocrystals. There are functional groups $-NH_2$ and $-COOH$ on the L-tryptophan molecules. Because the p*I* of L-tryptophan is 5.89 and the pH of the reaction solution is 6.3, there is electrostatic attraction between the positively charged $Cu^{2\pm}$ ion and the negatively charged carboxylic groups of L-tryptophan when $Cu^{2\pm}$ ions enter into aqueous solution, thus forming complex $Cu^{2\pm}$-tryptophan. Upon the introduction of I^{-}, the redox reaction between Cu^{2+}-tryptophan and I^{-} results in the formation of CuI crystal seeds (Scheme 1B). Under the reaction condition, L-tryptophan would preferentially adsorb on the {1 1 1} facets and consequently suppress the growth in the {1 1 1} direction. Thus, triangular-shaped seeds were formed [43]. Once a wrapping layer is established on the triangular-shaped seeds, it directs the growth of another layer, forming steps and corrugated edges in the process. During the reaction process, the reaction rate is expected to decrease because of reactant depletion, the deposition of CuI then follow the most energetically favorable path, the steps be leveled, and the edges be smoothened (Scheme 1C) [44]. Second, according to the theory developed by Israelachvili [45], when the concentration of surfactant or additive is above a certain "critical" value, the assembly will happen and the morphology

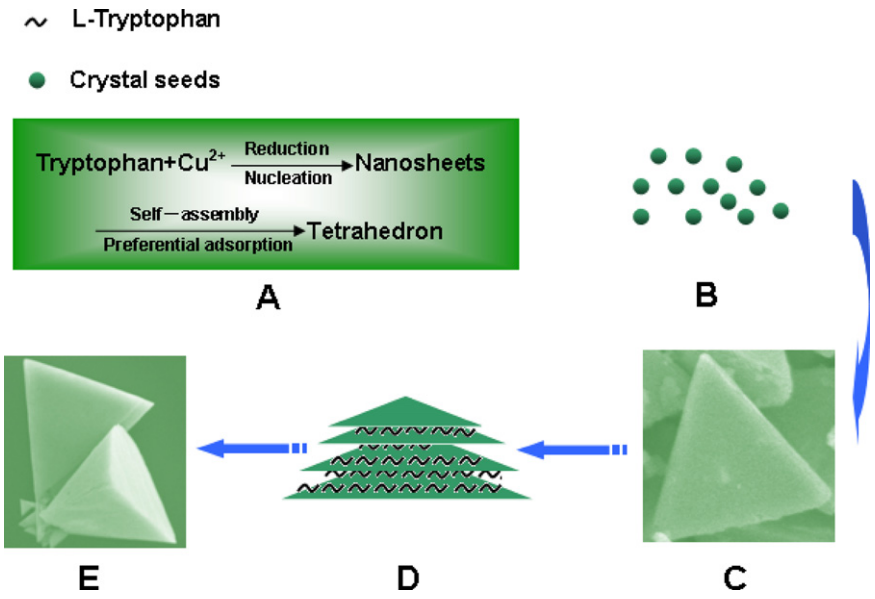

Scheme 1. Schematic illustration of the proposed formation mechanism for the as-obtained hierarchically micro/nano-structured CuI tetrahedron. (A) Simple representation of the formation of tetrahedron, (B) the formation of CuI crystal seeds, (C) the formation of triangular nanosheets, (D) the self-assembly of nanosheet, (E) formation of nanosheet-based tetrahedron.

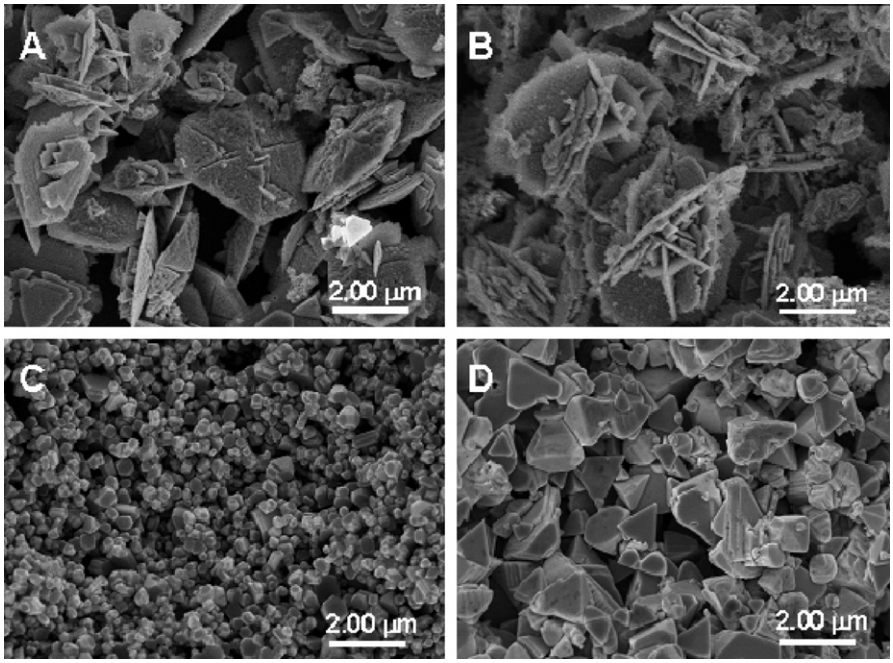

Fig. 4. FESEM image of the products: (A) the volume ratio of $CuSO_4$ to L-tryptophan is 1:1; (B) the volume ratio of $CuSO_4$ to L-tryptophan is 1:1.6; (C) substituting ascorbic acid for L-tryptophan; and (D) substituting sodium citrate for L-tryptophan.

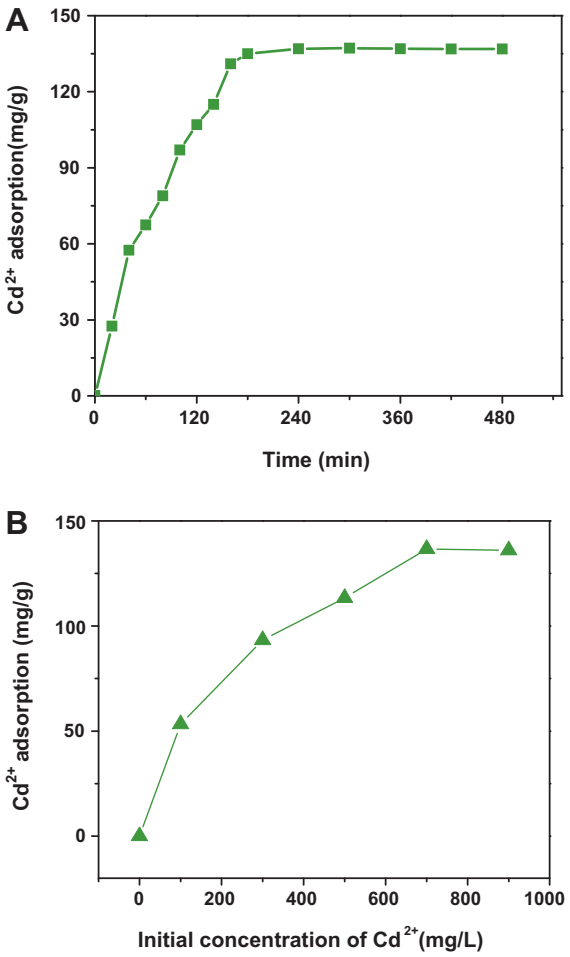

Fig. 5. (A) The effect of contact time on the adsorption amount of Cd(II) ions. (B) Adsorption isotherm of Cd(II) on the as-prepared hierarchically micro/nano-structured CuI tetrahedron at 25 °C.

depends on the well-known packing parameter $P = V/l_c a_0$, where V and l_c are the volume and chain length of the hydrophobic group, respectively, and a_0 is the cross-sectional area of the headgroup dictated by the electrostatic repulsion between adjacent headgroups in the associates. Reducing the electrostatic repulsion between adjacent headgroups can increase the packing factor P, and facilitate assembly (Scheme 1D). This speculation is supported by the control experiments by varying the volume ratio of L-tryptophan to $CuSO_4$. As shown in Fig. 4, with the decrease of the volume ratio of L-tryptophan to $CuSO_4$ from 1.7 to 1, the dimension of the product's morphology degrades from 3D tetrahedron (Fig. 3) to 2D hexagonal nanosheets (Fig. 3A). By increasing the molar ratio of L-tryptophan to $CuSO_4$ from 1 to 1.6, the dimension of the product's morphology evolved from 2D (Fig. 4A) to 3D (Fig. 4B). This may be ascribed to that the larger volume ratio of L-tryptophan to $CuSO_4$, the higher possibility that the headgroups of L-tryptophan is compressed, the larger value of P, and the higher possibility the assembly [46]. Third, it is generally accepted that for a face-centred-cubic (fcc) single crystal, surface energies associated with different crystallographic planes are usually different, and a general sequence may hold $\gamma(1\,1\,1) < \gamma(1\,0\,0) < \gamma(1\,1\,0)$. In our case, L-tryptophan molecules tend to preferentially adsorb on the {1 1 1} planes during the reaction, consequently the ratio R increases. On the other hand, according to Gibbs–Curie–Wulff theorem, tetrahedron is associated with the maximal stability among the polygonal structures [47]. All these factors are combined together in our system and thus hierarchically micro/nano-structured tetrahedron is constructed with the assistance of a biomolecule such as L-tryptophan.

As it is well known, when Cu^{2+} and I^- are mixed in water solution at room temperature, a redox reaction occurs immediately and irregular CuI microparticles and brown iodine solution form. In the presence of L-tryptophan, however, a colorless solution is produced, which proves that L-tryptophan itself is responsible for this reduction reaction. Besides, the failure to produce tetrahedral CuI when substituting ascorbic acid (Fig. 4C) and sodium citrate (Fig. 4D) for L-tryptophan further confirms the morphology-directing role of L-tryptophan in the formation of such unique tetrahedral CuI. All these observations give a

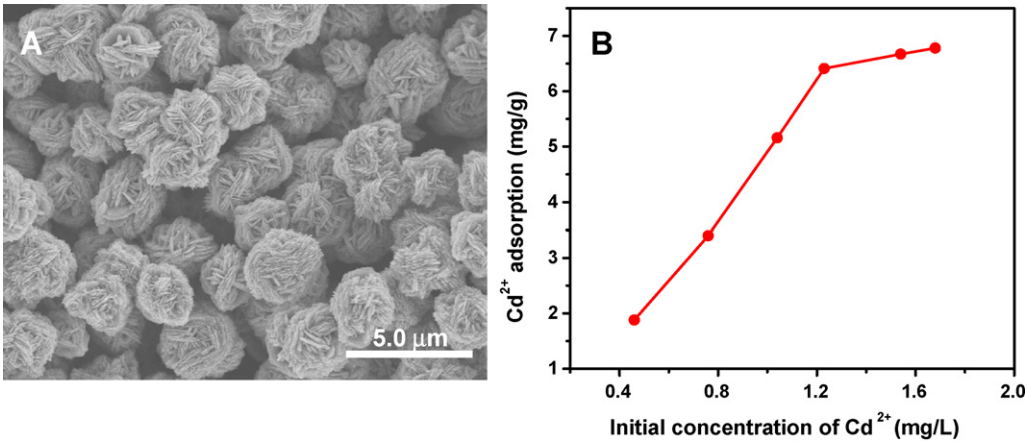

Fig. 6. (A) The FESEM images of the CuO microspheres. (B) Adsorption isotherm of Cd(II) on the CuO microspheres at 25 °C.

firm proof for the application of biomolecules in nanomaterial synthesis.

3.3. Cd(II) removal

The as-formed hierarchically micro/nano-structured CuI tetrahedron is expected to possess high specific surface area, therefore enhancing accessibility of adsorbates to the reactive sites, as demonstrated here as adsorbent for heavy metal Cd(II) ions. In Fig. 5A, adsorption of Cd(II) by CuI indicated rapid binding of Cd(II) initially, however with the passage of time adsorption rate slowed down. Equilibrium reached at 4 h, no change in the uptake capacity was observed up to 8 h. Thus, a total of 4 h is selected to attain equilibrium. Then the heavy metal ions adsorption by CuI sample was given as a function of initial concentration of Cd(II) ions within the aqueous phase in Fig. 5B. The Cd(II) removal capacity was determined to be 136.3 mg/g based on Langmuir simulation [36]. Compared with the Cd(II) removal capacities of amidoximated polyacrylonitrile/organobentonite composite (52.61 mg/g) [48], porous poly(methyl methacrylate) beads (24.2 mg/g) [49], and nettle ash (142.8 mg/g) [18], the as-prepared CuI sample shows promising potential for industrial application as adsorbent for Cd(II). Although it is lower than the maximum sorption capacity of γ-cyclodextrin/chitosan composites, 833.33 mg/g [19], the facile and cost-effective synthesis of the adsorbent may to some extent compensate for it in our case.

The regeneration of the adsorbent is believed to be a key factor in improving process economics. Desorption studies were carried out using Y solution. Almost 98% of the adsorbed Cd(II) was recovered after the first cycle. The desorption efficiencies were 96% and 95%, respectively, for the next two cycles. The significant desorption can be attributed to the adsorption mechanism. There are two well-established adsorption mechanisms. One is a physical one, and the other is a chemical one. Most of the adsorbents for Cd^{2+} are mainly based on physical mechanisms. In our case, I^- ions behave as active adsorption sites. The high affinity of Cd(II) to I^- is expected to result in the formation of stable CdI_4^{2-}, induce the great decrease of $Cd^{2\pm}$ in the solution, and therefore the as-prepared CuI sample showed high removal capacity for Cd(II). The adsorption should be ascribed to a chemical one, quite different from physical adsorption for removing Cd(II) [50,51]. In order to release the active adsorption sites, other ligands with higher affinity to Cd(II) should be utilized to decomplex the stable CdI_4^{2-}. It is well-known that the formation constant between Cd(II) and Y of CdY^{2-}, 4.0×10^{16}, is significantly larger than that of CdI_4^{2-}, 2.6×10^5 [52]. So the introduction of Y to the adsorption system is expected to produce CdY^{2-}, release I^- ions, and reactivate reactive adsorption sites. The overall chemical adsorption/desorption process can be formulated based on chemical adsorption mechanism, shown as in Eqs. (3)–(6). The better mechanical and structure stability of the hierarchically micro/nano-structured materials than that of nano-sized materials greatly help the recycle performance.

In order to confirm this chemical-adsorption-based mechanism, we carried out the adsorption test by substituting micro/nano-structured CuI tetrahedron by CuO microspheres prepared according to our previous work [53]. Fig. 6A showed that the CuO microspheres feature hierarchical micro/nanostructure. Fig. 6B shows a typical adsorption isotherm of Cd(II) on the CuO microspheres at 25 °C measured with different initial Cd(II) concentrations. The Cd(II) removal capacity is analyzed to be 6.67 mg/g. In contrast, the as-prepared CuI sample shows performance as adsorbent for Cd(II). The difference between CuI and CuO lies in I^- and O^{2-}, so the assumption that the adsorption should be ascribed to a chemical one in the case of CuI is reasonable and acceptable.

$$CuI \Leftrightarrow Cu^+ + I^- \quad (3)$$

$$Cd^{2+} + 4I^- \Leftrightarrow CdI_4^{2-} \quad (4)$$

$$CdI_4^{2-} + Y^{4-} \Leftrightarrow CdY^{2-} + 4I^- \quad (5)$$

$$Cu^+ + I^- \Leftrightarrow CuI \quad (6)$$

4. Conclusion

In summary, we have succeeded in synthesizing hierarchically micro/nano-structured CuI tetrahedron via biomolecule-assisted assembly from nanosheets at room temperature in short time. Here, a biomolecule such as L-tryptophan biomolecule, L-tryptophan plays dual roles, namely as reducing and morphology-directing agents, in the formation of the product. The procedure that we describe here is a green, environment-friendly, efficient, and direct one-step process for the preparation of hierarchically micro/nano-structured tetrahedron. Compared with the nano-sized materials, the as-formed hierarchically tetrahedral micro/nano-structure has improved mechanical and structural stability. It guarantees its excellent recycle performance on adsorption, as demonstrated here for applications as recyclable adsorbents for Cd(II) with high removal capacity. Surely, the chemical adsorption mechanism, in addition to hierarchical micro/nano-structure, plays a vital role in the excellent Cd(II) removal performance. Parallelly, this report is also a good example for the organic combination of bioinspired synthesis and functional materials.

Acknowledgments

The authors are grateful to the editor and referees for their constructive comments and suggestions. This work was supported by the National Natural Science Foundation of China (21071047), Program for New Century Excellent Talents in University (NCET), the Project Sponsored by the Scientific Research Foundation for the Returned Overseas Chinese Scholars, State Education Ministry of China, Excellent Youth Foundation of He'nan Scientific Committee, and the Program for Science & Technology Innovation Talents in Universities of Henan Province (2011HASTIT010).

References

[1] K. Selvaraj, S. Manonmani, S. Pattabhi, Ingenta connect removal of hexavalent chromium using distillery sludge, Bioresour. Technol. 89 (2003) 207–211.
[2] S.B. Akar, G. Asli, A. Burcu, K. Zerrin, A. Tamer, Investigation of the biosorption characteristics of lead (II) ions onto symphoricarpus albus: batch and dynamic flow studies, J. Hazard. Mater. 165 (2009) 126–133.
[3] N. Yasar, M. Emine, Thermodynamic and kinetic studies for environmentally friendly Ni(II) biosorption using waste pomace of olive oil factory, Bioresour. Technol. 100 (2009) 2375–2380.
[4] T.K. Naiyaa, A.K. Bhattacharyaa, S.K. Das, Adsorption of Cd(II) and Pb(II) from aqueous solutions on activated alumina, J. Colloid Interface Sci. 333 (2009) 14–26.
[5] S. Parinda, N. Akira, T. Paitip, B. Yoshinari, N. Wonranan, Mechanism of Cr(VI) adsorption by coir pith studied by ESR and adsorption kinetic, J. Hazard. Mater. 161 (2009) 1103–1108.
[6] M.P. Waalkes, Cadmium carcinogenesis in review, J. Inorg. Biochem. 79 (2000) 241–244.
[7] E.C. Foulkes, Biological Effects of Heavy Metals, CRC Press, Boca Raton, FL, 1990.
[8] J. Anwar, U. Shafique, W. Zaman, M. Salman, A. Dar, S. Anwar, Removal of Pb(II) and Cd(II) from water by adsorption on peels of banana, Bioresour. Technol. 101 (2010) 1752–1755.
[9] Q. Cristina, R. Zelia, F. Bruna, F. Hugo, T. Teresa, Biosorptive performance of an *Escherichia coli* biofilm supported on zeolite NaY for the removal of Cr(VI), Cd(II), Fe(III) and Ni(II), Chem. Eng. J. 152 (2009) 110–115.
[10] N. Muhammad, A. Mahmood, S.A. Shahid, S.S. Shah, A.M. Khalid, G. McKay, Sorption of lead aqueous solution by chemically modified carbon adsorbents, J. Hazard. Mater. 138 (2006) 604–613.
[11] S. Ahmet, T. Mustafa, Biosorption of total chromium from aqueous solution by red algae 9ceramium virgatum: equillibrium, kinetic and thermodynamic studies, J. Hazard. Mater. 160 (2008) 349–355.
[12] K.N. Tarun, C. Pankaj, K.B. Ashim, K.D. Sudip, Saw dust and neem bark as low cost natural biosorbebt for adsorptive removal of Zn(II) and Cd(II) ions form aqueous solutions, Chem. Eng. J. 148 (2008) 68–79.
[13] V.B.H. Dang, H.D. Doan, T. Dang-Vu, A. Lohi, Equilibrium and kinetics of biosorption of cadmium (II) and copper(II) by wheat straw, Bioresour. Technol. 100 (2009) 211–219.
[14] S. Suresh, V.C. Srivastava, I.M. Mishra, Isotherm, thermodynamics, desorption and disposal study for the adsorption of catechol and resorcinol onto granular activated carbon, J. Chem. Eng. Data 56 (2011) 811–818.
[15] L. Canet, M. Ilpide, P. Seta, Efficient facilitated transport of lead, cadmium, zinc and silver across a flat sheet-supported liquid membrane mediated by lasalocid A, Sep. Sci. Technol. 37 (2002) 1851–1860.
[16] O.J. Esalah, M.E. Weber, J.H. Vera, Removal of lead, cadmium and zinc from aqueous solutions by precipitation with sodium di-(*n*-octyl) phosphinate, Can. J. Chem. Eng. 78 (2000) 948–954.
[17] Y. Jiang, S. Gao, Z. Li, X. Jia, Y. Chen, Cauliflower-like CuI nanostructures: green synthesis and applications as catalyst and adsorbent, Mater. Sci. Eng. B 176 (2011) 1021.
[18] H.Z. Mousavi, S.R. Seyedi, Nettle ash as a low cost adsorbent for the removal of nickel and cadmium from wastewater, Int. J. Environ. Sci. Technol. 8 (2011) 195–202.
[19] A.K. Mishra, A.K. Sharma, Synthesis of γ-cyclodextrin/chitosan composites for the efficient removal of Cd(II) from aqueous solution, Int. J. Biol. Macromol. 49 (2011) 504–512.
[20] J.W. Patterson, Wastewater Treatment Technology, Ann Arbor Inc., New York, 1975.
[21] D. Feng, J.S.J. Deventer, C. Aldrich, Removal of pollutants from acid mine wastewater using metallurgical by-product slags, Sep. Purif. Technol. 40 (2004) 61–67.
[22] K.K. Panday, G. Prasad, V.N. Singh, Removal of Cr(VI) from aqueous solutions by adsorption on fly ash-wollastonite, J. Chem. Technol. Biotechnol. 34A (1984) 367–374.
[23] B. Bayat, Comparative study of adsorption properties of Turkish fly ashes: II. The case of chromium(VI) and cadmium(II), J. Hazard. Mater. 95 (2002) 275–290.
[24] G. Suraj, C.S.P. Iyer, M. Lalithambika, Adsorption of cadmium and copper by modified kaolinites, Appl. Clay Sci. 13 (1998) 293–306.
[25] L.S. Zhong, J.S. Hu, H.P. Liang, A.M. Cao, W.G. Song, L.J. Wan, Self-assembled 3D flowerlike iron oxide nanostructures and their application in water treatment, Adv. Mater. 18 (2008) 2426–2431.
[26] L.S. Zhong, J.S. Hu, A.M. Cao, Q. Liu, W.G. Song, L. Wan, 3D flowerlike ceria micro/nanocomposite structure and its application for water treatment and CO removal, Chem. Mater. 19 (2007) 1648–1655.
[27] J.S. Hu, L.S. Zhong, W.G. Song, L.J. Wan, Synthesis of hierarchically structured metal oxides and their application in heavy metal ion removal, Adv. Mater. 20 (2008) 2977–2982.
[28] S. Gao, Z. Li, K. Jiang, H. Zeng, L. Li, X. Fang, X. Jia, Y. Chen, Biomolecule-assisted in situ route toward 3D superhydrophilic Ag/CuO micro/nanostructures with excellent artificial sunlight self-cleaning performance, J. Mater. Chem. 21 (2011) 7281–7288.
[29] S. Gao, H. Zhang, X. Wang, R. Deng, D. Sun, G. Zheng, ZnO-based hollow microspheres: biopolymer-assisted assemblies from ZnO nanorods, J. Phys. Chem. B 110 (2006) 15847–15852.
[30] S. Gao, H. Zhang, R. Deng, X. Wang, D. Sun, G. Zheng, Engineering white light-emitting Eu-doped ZnO urchins by biopolymer-assisted hydrothermal method, Appl. Phys. Lett. 89 (2006) 123125-1–1123125-3.
[31] Y. Zhou, M. Kogiso, M. Asakawa, S. Dong, R. Kiyama, T. Shimizu, Antimicrobial nanotubes consisting of Ag-embedded peptidic lipid-bilayer membranes as delivery vehicles, Adv. Mater. 21 (2009) 1742–1745.
[32] J.P. Xie, Y.G. Zheng, J.Y. Ying, High yield preparation of macroscopic graphene oxide membranes, J. Am. Chem. Soc. 131 (2009) 888–889.
[33] J.P. Xie, Y.G. Zheng, J.Y. Ying, Highly selective and ultrasensitive detection of Hg^{2+} based on fluorescence quenching of Au nanoclusters by Hg^{2+}–Au^{+} interactions, Chem. Commun. 46 (2010) 961–963.
[34] N. Ma, A.F. Marshall, J.H. Rao, Near-infrared light emitting luciferase via biomineralization, J. Am. Chem. Soc. 132 (2010) 6884–6885.
[35] Y.Z. Wu, S. Chakrabortty, R.A. Gropeanu, J. Wilhelmi, Y. Xu, K.S. Er, S.L. Kuan, K. Koynov, Y. Chan, T. Weil, pH-responsive quantum dots via an albumin polymer surface coating, J. Am. Chem. Soc. 132 (2010) 5012–5014.
[36] S. Hasan, A. Krishnaiah, T.K. Ghosh, D.S. Viswanath, V.M. Boddu, E.D. Smith, Ind. Eng. Chem. Res. 45 (2006) 5066–5077.
[37] P.D. Kirsch, J.G. Ekerdt, Chemical and thermal reduction of thin films of copper (II) oxide and copper (I) oxide, J. Appl. Phys. 90 (2001) 4256–4264.
[38] W.R. Salaneck, H.R. Thomas, R.W. Bigelow, C.B. Duke, E.W. Plummer, A.J. Heeger, A.G. Macdiarmid, Photoelectron spectroscopy of iodine-doped polyacetylene, J. Chem. Phys. 72 (1980) 3674–3678.
[39] G. Polzonetti, V. Faruffini, A. Furlani, M.V. Russo, X-ray photoelectron spectroscopy study of the interaction with iodine doped polyethynylferrocene, Synth. Met. 29 (1989) 495–499.
[40] Y.G. Sun, Y.N. Xia, Shape-controlled synthesis of gold and silver nanoparticles, Science 298 (2002) 2176–2179.
[41] B.J. Wiley, Y.J. Xiong, Z.Y. Li, Y.D. Yin, Y.N. Xia, Right bipyramids of silver: a new shape derived from single twinned seeds, Nano Lett. 6 (2006) 765–768.
[42] A. Tao, P. Sinsermsuksakul, P.D. Yang, Polyhedral silver nanocrystals with distinct scattering signatures, Angew. Chem. Int. Ed. 45 (2006) 4597–4601.
[43] J. Xie, J.Y. Lee, D.I.C. Wang, Identification of active biomolecules in the high-yield synthesis of single-crystalline gold nanoplates in algal solutions, J. Phys. Chem. C 111 (2007) 10226–10232.
[44] J. Feng, H.C. Zeng, Size-controlled growth of Co_3O_4 nanocubes, Chem. Mater. 15 (2003) 2829–2835.
[45] J.N. Israelachvili, Intermolecular and Surface Forces, Academic Press, New York, 1992.
[46] L.M. Zhai, M. Zhao, D.J. Sun, J.C. Hao, L.J. Zhang, Salt-induced vesicle formation from single anionic surfactant SDBS and its mixture with LSB in aqueous solution, J. Phys. Chem. B 109 (2005) 5627–5630.
[47] C.H.B. Ng, W.Y. Fan, Facile synthesis of single-crystalline γ-CuI nanotetrahedrons and their induced transformation to tetrahedral CuO nanocages, J. Phys. Chem. C 111 (2007) 9166–9171.
[48] T.S. Anirudhan, M. Ramachandran, Synthesis and characterization of amidoximated polyacrylonitrile/organobentonite composite for Cu(II), Zn(II), and Cd(II) adsorption from aqueous solutions and industry wastewaters, Ind. Eng. Chem. Res. 47 (2008) 6175–6184.
[49] A. Denizli, N. Sanli, B. Garipcan, S. Patir, G. Alsancak, Methacryloylamidoglutamic acid incorporated porous poly(methyl methacrylate) beads for heavy-metal removal, Ind. Eng. Chem. Res. 43 (2004) 6095–6101.
[50] K. Kadirvelu, K. Thamaraiselvi, C. Namasivayam, Removal of heavy metals from industrial wastewaters by adsorption onto activated carbon prepared from an agricultural solid waste, Bioresour. Technol. 76 (2001) 63–65.
[51] L.V.A. Gurgel, R.P. Freitas, L.F. Gil, Adsorption of Cu(II), Cd(II), and Pb(II) from aqueous single metal solutions by sugarcane bagasse and mercerized sugarcane bagasse chemically modified with succinic anhydride, Carbohydr. Polym. 74 (2008) 922–929.
[52] X.Z. Cao, T.Y. Song, X.Q. Wang, Inorganic Chemistry, 3th ed., High Education Press, Beijing, 1994.
[53] S. Gao, S. Yang, J. Shu, S. Zhang, Z. Li, K. Jiang, Green fabrication of hierarchical CuO hollow micro/nanostructures and enhanced performance as electrode materials for lithium-ion batteries, J. Phys. Chem. C 112 (2008) 19324–19328.